Analysis and Optimization of Impact Resistance Performance of Variable Gradient Corrugated Sandwich Structure

Wang Tingting, Wang Qi*, Li Zhongqiu

College of Aeronautics and Astronautics, Nanchang Hangkong University, Nanchang 330063, China

Abstract: Corrugated sandwich structures, known for their exceptional specific stiffness, specific strength, lightweight characteristics, and superior energy absorption capabilities, are extensively used in the structural design of aerospace equipment. Given that aerospace equipment structures are prone to external impact loads during use, and considering the high demands for ensuring the safety of equipment and personnel, as well as the reliability of structural components, it is imperative to enhance the impact resistance of equipment structures. This paper introduces a novel biomimetic variable gradient corrugated sandwich structure based on biomimetic principles and constructs finite element models of five different gradient distributions of corrugated sandwich structures under impact loads using numerical simulation technology. The study systematically analyzes the influence of gradient distribution on the impact resistance of corrugated sandwich structures. The research reveals that the biomimetic corrugated sandwich structure with a 3-6-3 variable gradient distribution exhibits excellent impact resistance, offering a new design approach for more efficient anti-impact equipment structures. The study further investigates the impact of sandwich structural parameters on the impact resistance of corrugated sandwich structures and employs genetic algorithms for structural parameter optimization. The results indicate that the optimized corrugated sandwich structure panels not only achieve a significant enhancement in impact resistance but also realize structural lightweighting.

Keywords: Variable Gradient Corrugated Sandwich Structures; Impact Resistance; Bionic; Optimization

DOI: 10.57237/j.mse.2024.03.002

1 Introduction

Sandwich structures, known for their high specific strength, high specific stiffness, and excellent energy absorption capabilities, are widely used as protective components, particularly in defense, aerospace, automotive, and marine industries. In the aerospace field, aircraft wings and cowling skins, which are predominantly sandwich structures, are often subjected to impacts from bird strikes, hail impacts, small stone hits, and tool drops during maintenance. These impacts can cause local dents and damage to the aircraft structural components, significantly reducing the stiffness and residual strength of the aircraft structure, thereby posing a serious threat to the safety of the aircraft [1]. Therefore, an in-depth study of the impact resistance performance of sandwich structures under foreign object impacts is of significant engineering value and practical importance for ensuring aircraft structural safety, extending service life, and reducing maintenance costs.

In recent years, sandwich structures have been rapidly and widely adopted across various fields due to their unique mechanical properties. Their impact resistance, a

Funding: National Natural Science Foundation of China (12362026).

*Corresponding author: Wang Qi, wangqi439@126.com

Received: 19 November 2024; Accepted: 24 December 2024; Published Online: 9 January 2025 http://www.mechscieng.com

critical indicator of structural safety, has garnered significant interest from experts and scholars worldwide. Current research on sandwich structures primarily focuses on the impact of different structural configurations, punch shapes, and impact angles on their impact resistance [2-8]. However, there is a relative scarcity of research on the impact resistance of gradient-varying sandwich structures. Consequently, this study employs finite element analysis simulation software to numerically simulate the dynamic response of variable gradient sandwich structures under impact loading. It analyzes key parameters affecting the structural impact mechanics, aiming to provide a reference for the impact resistance assessment of sandwich structures.

2 Structure Design and Numerical Calculation Model Establishment

2.1 Sandwich Structure Design

Biological organisms in nature have served as a muse for the design of novel sandwich structures that exhibit low density, high strength, and exceptional energy absorption capabilities. A prime example is the mantis shrimp's raptorial claw, which can apply considerable force and velocity to fracture the shells of mollusks or other rigid structures with ease, achieving a maximum impact force of 1500N without incurring catastrophic failure [9]. Studies have demonstrated that the raptorial claw of the mantis shrimp is capable of withstanding high-intensity impacts and efficiently absorbing impact energy through its inherent structure, t-hereby showcasing high strength and superior impact resistance characteristics [10]. Microstructural observations of the impact-resistant region within the raptorial claw (Figure 1) [11] reveal periodic sinusoidal patterns aligned with the direction of the applied load, with a gradient variation distribution observed among these sinusoidal structures. Based on these observations, this study has adopted a sinusoidal structure in the coreconfiguration design and has conducted a gradient variation structure design for the corrugated sandwich panel. The mathematical expression for the sinusoidal curve is given by

$$y=A*\sin(B*x) \tag{1}$$

In Equation (1), A represents the amplitude of the sinusoidal function, and B represents the wave number. To examine the effects of gradient variation on the impact resistance of corrugated sandwich structures, five distinct gradient-varied structures were designed while keeping the overall height and the wave number B constant across all layers. The amplitude A of each sinusoidal layer was adjusted to create these variations, as illustrated in Figure 2. The nomenclature 3-4-5 indicates the amplitudes of the upper, middle, and lower sinusoidal core layers are 3 mm, 4 mm, and 5 mm, respectively, with each layer being separated by flat panels.

(a) Mantis shrimp appearance figure

(b) Mantis shrimp raptorial claw microstructure

Figure 1 Mantis shrimp raptorial claw structure

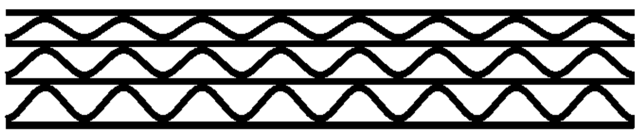

(a) 3-4-5 increasing gradient distribution

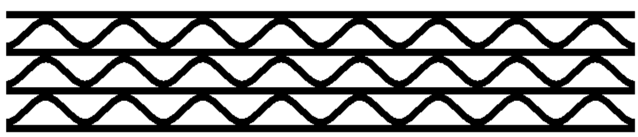

(b) 4-4-4 horizontal gradient distribution

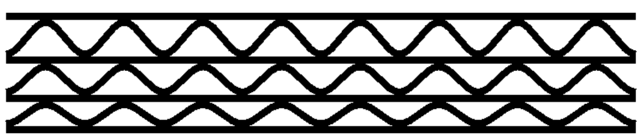

(c) 5-4-3 decreasing gradient distribution

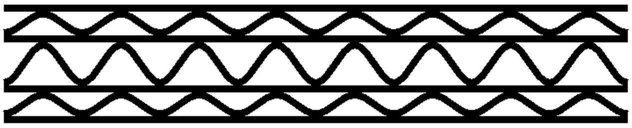

(d) 3-6-3 increasing then decreasing gradient distribution

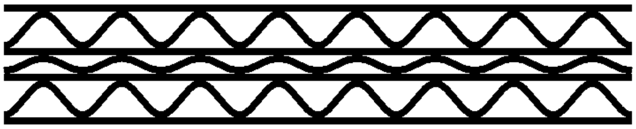

(e) 5-2-5 decreasing then increasing gradient distribution

Figure 2 Gradient distribution of ripple core structure

2.2 Finite Element Numerical Calculation Model

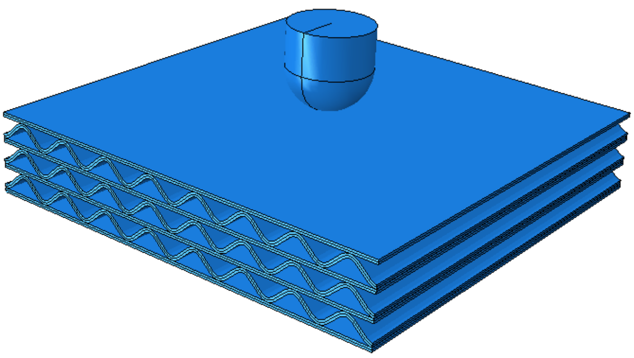

Figure 3 Variable gradient ripple core structure local impact finite element model

This paper employs the commercial finite element software Abaqus to conduct a local impact finite element analysis of the corrugated sandwich structure, as depicted in Figure 3. The overall dimensions of the corrugated sandwich structure are 100mm×100mm×12mm, and the mass of the impactor is 2.5kg, shaped as a combination of a hemisphere and a cylinder, with the cylinder's diameter being 10mm. During the simulation, both the corrugated sandwich structure and the impactor are modeled using shell elements. To ensure the accuracy and convergence of the model, a 5-point integration is used in the thickness direction of the elements. The boundary nodes of the corrugated sandwich structure are fully constrained, and 'Tie' constraints are used to connect the face sheets and the core, ensuring the structural integrity. The impactor is defined as a rigid body and impacts the corrugated sandwich structure at a speed of 5 m/s. The contact between the rigid impactor and the corrugated sandwich structure is set as surface-to-surface contact, with a tangential friction coefficient of 0.2, and the normal contact is defined as a hard contact. The face sheets and the core of the corrugated sandwich structure are made of aluminum alloy, and their basic material parameters are shown in Table 1.

Table 1 Aluminum alloy material properties

Density/(kg/m^3)	Elastic modulus/(GPa)	Poisson ratio
2.77×10^3	71	0.33

2.3 Mesh Independence Verification of Numerical Models

The size of finite element meshes significantly affects the computational accuracy and required computational resources of a model. An oversized mesh may lead to a decrease in computational accuracy, while an undersized mesh can increase computational costs and time. Therefore, selecting an appropriate mesh size is crucial for ensuring computational precision and efficiency. To balance the computational accuracy and computational time of the model, this study conducted a mesh independence verification on the numerical model, employing four different mesh sizes of 3mm×3mm, 2mm×2mm, 1mm×1mm, and 0.9mm×0.9mm f-or simulation calculations. Figure 4 shows that when the mesh size is refined to 0.9mm×0.9mm, the simulation results of the model are very close to those of the 1mm×1mm mesh, with the time-kinetic energy curves almost coinciding. Therefore, this study selected a mesh size of 1mm×1mm for meshing the corrugated sandwich structure to achieve the optimal balance between computational efficiency and accuracy.

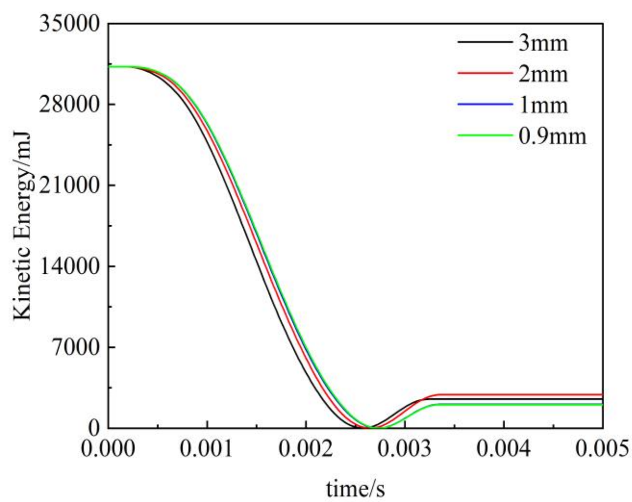

Figure 4 Kinetic energy-time curves of the model impactor at different mesh sizes

3 Analysis of Simulation Results

3.1 Research on Corrugated Core Structures with Different Gradient Variations

Under identical impact loads, corrugated sandwich structures with different gradient distributions exhibit varying impact resistance performance. As depicted in Figure 5, the impact response curves of five corrugated sandwich structures with varying gradient distributions under the same impact load reveal these performance differences.

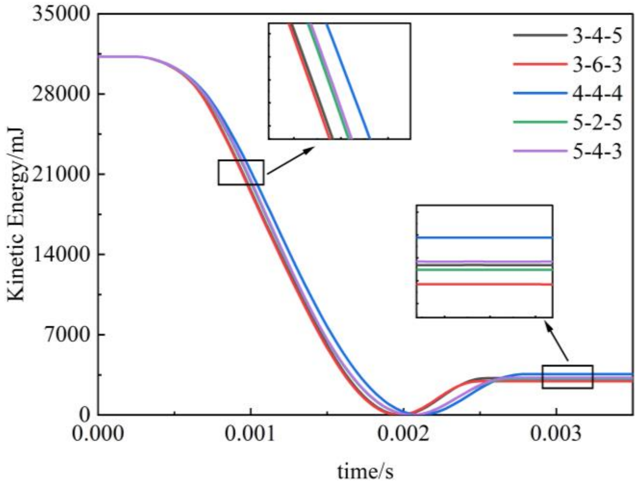

(a) Kinetic energy-time curves of impactor with different gradient distributions

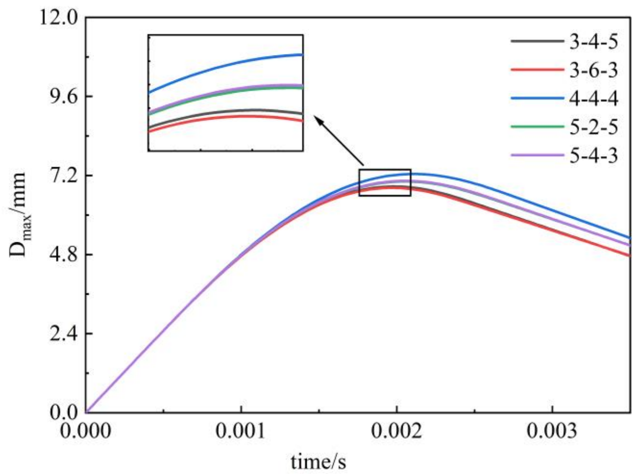

(b) Displacement-time curves of maximum displacement with different gradient distributions

Figure 5 Impact response curves of corrugated sandwich panels with different gradient distributions

Examination of the curve in Figure 5(a) allows us to categorize the kinetic energy variation of the impactor into three distinct phases: In the first phase, prior to contact with the corrugated sandwich structure, the impactor maintains its maximum kinetic energy. In the second phase, as time progresses, the impactor begins to move in the vertical direction along the structure. At approximately 0.0005 seconds, the impactor makes contact with the corrugated sandwich structure, and its kinetic energy starts to decrease. By the time it reaches 0.002 seconds, the impactor's kinetic energy is converted into internal energy and frictional dissipation within the corrugated sandwich structure, dropping to zero as the impactor reaches its maximum downward displacement, thus concluding the second phase. In the third phase, after the impactor's kinetic energy has dropped to zero, the structure, not being completely destroyed by the impact load, begins to rebound, causing the impactor's kinetic energy to increase again. Once the structure rebounds to a certain extent, the impactor's kinetic energy stabilizes. The greater the remaining kinetic energy of the impactor at this point, the less energy the impacted structure has absorbed during the impact; conversely, the more energy it has absorbed. Figure 5(a) illustrates that throughout the entire impact process on the corrugated sandwich structure, the impactor of the structure with a 3-6-3 gradient distribution has the least remaining kinetic energy, indicating that increasing the amplitude of the middle core layer is beneficial for energy absorption efficiency.

Examination of the curve in Figure 5(b) reveals that the displacement-time curve of the corrugated sandwich structure is approximately parabolic. The displacement change can be divided into two stages: the ascending and descending phases. During the ascending phase, as time increases, the impactor's downward displacement continues to rise, reaching its peak at 0.002 seconds, which signifies the maximum downward displacement of the structure. Subsequently, the curve enters the descending phase. When the impactor reaches its maximum downward displacement, its impact velocity drops to zero, and most of its kinetic energy is converted into the structure's internal energy. The structure then undergoes rebound deformation, and the impactor moves in the opposite direction of the impact, with the curve change being less steep compared to the ascending phase. Figure 5(b) indicates that throughout the entire impact process, the corrugated sandwich structure with a 3-6-3 gradient variation has the smallest maximum downward displacement of the impactor, suggesting that increasing the amplitude of the middle core layer is beneficial for enhancing the structure's resistance to deformation.

3.2 Parametric Study of Variable Gradient Corrugated Sandwich Structures

Based on the performance analysis of corrugated sandwich structures under identical load impacts in the previous section, it was observed that structures with larger amplitudes in the middle layer exhibit superior energy absorption and greater resistance to deformation. Consequently, this section adopts the 3-6-3 gradient distribution corrugated sandwich structure as the impact model to further investigate the influence of structural parameters on its impact resistance performance.

In this study, two key parameters are defined to assess the impact resistance performance of the corrugated sandwich structure: SEA and D_{max}. SEA represents the structure's lightweight energy absorption capability, that is, the energy absorption per unit mass, and is calculated using the following formula [12]:

$$SEA = \frac{E}{M} \tag{2}$$

where E denotes the energy absorbed by the structure during the impact, and M denotes the total mass of the structure.

3.2.1 The Impact of Punch Impact Location on Structural Impact Resistance Performance

The impact resistance performance of a structure is influenced by the location of the impact during the impact process. This study conducted impact load simulations on the crest and trough positions of the corrugated sandwich structure to evaluate the effect of impact location on the structure's impact resistance performance. The simulation results indicate significant differences in the impact resistance performance at different impact locations, as shown in Figure 6.

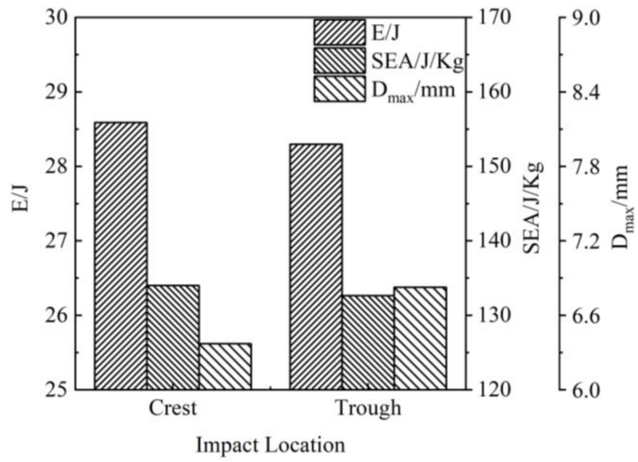

Figure 6 Effect of impact position on impact resistance of corrugated sandwich structure

Figure 6 presents a comparison of the impact resistance performance of the corrugated sandwich structure at the crest and trough positions. Analysis reveals that at the crest impact location, the structure absorbs more energy, exhibits higher SEA, and experiences a smaller maximum downward displacement of the impactor. This is attributed to the fact that at the crest impact location, both the face sheets and the core participate in the deformation, leading to greater energy absorption by the structure. Consequently, due to the support provided by the core, the structure undergoes less deformation, resulting in a reduced maximum downward displacement of the impactor. It can be concluded that when the impactor strikes the corrugated sandwich structure at the crest position, the structure demonstrates better energy absorption and stronger resistance to deformation, thereby possessing superior impact resistance capabilities.

3.2.2 The Influence of the Order of Sandwich Structure on the Impact Resistance of the Structure

Under identical load impact conditions, the impact resistance performance of corrugated sandwich structures varies depending on the arrangement of the corrugations. This study conducted impact load simulations on both regularly corrugated and symmetrically corrugated sandwich structures to assess the influence of different corrugation sequences on the structure's impact resistance performance. The simulation results, which highlight significant differences in impact resistance between the two corrugation patterns, are presented in

Figure 7.

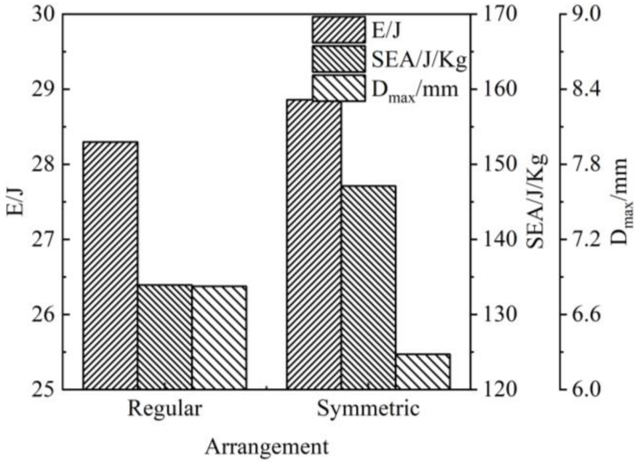

Figure 7 Effect of arrangement on impact resistance of corrugated sandwich structure

Figure 7 compares the impact resistance performance of symmetrically and regularly arranged corrugated sandwich structures under identical impact energy conditions. The results indicate that the symmetrically arranged corrugated sandwich structure absorbs more energy, has a higher *SEA*, and experiences a smaller maximum displacement of the impactor. This difference can be attributed to the mutual support between the cores in the symmetrical arrangement, which enhances the overall stiffness of the structure and thereby increases its resistance to deformation. Consequently, the symmetrically arranged corrugated sandwich structure demonstrates better energy absorption and stronger resistance to deformation, thereby improving its impact resistance performance.

3.2.3 Effect of Panel Thickness on Impact Resistance of Structure

This study aims to investigate the impact of face sheet thickness on the impact resistance performance of corrugated sandwich structures. To this end, impact load simulations were conducted on corrugated sandwich structures with varying face sheet thicknesses t_f while keeping the core thickness constant. The face sheet thicknesses were set to 0.6mm, 0.7mm, 0.8mm, 0.9mm, and 1mm. The simulation results elucidate the specific influence of face sheet thickness on the structural impact resistance performance, as depicted in Figure 8.

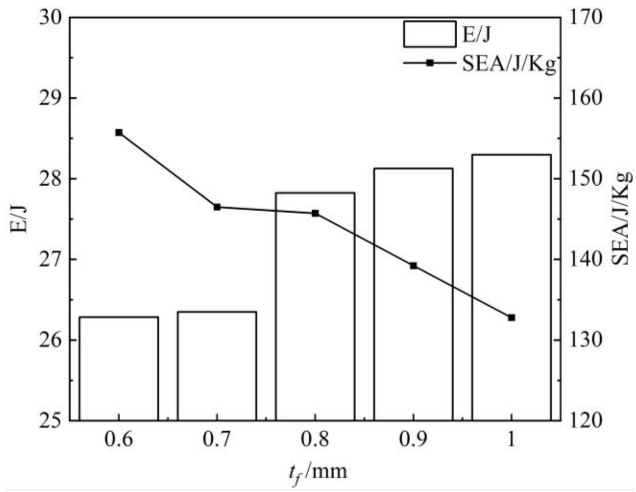

(a) Effect of panel thickness on energy absorption and specific energy absorption

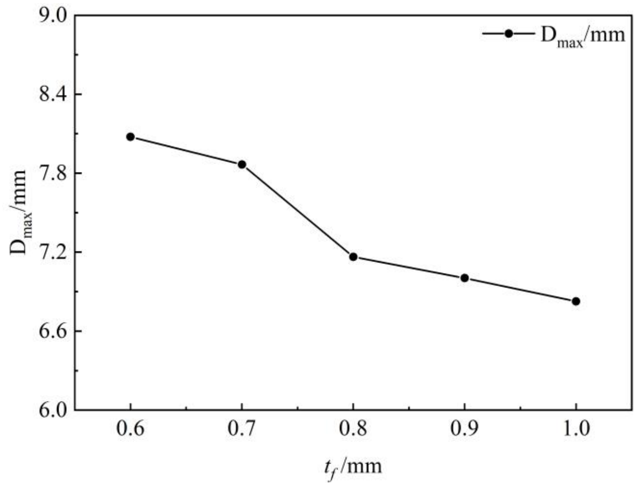

(b) The influence of panel thickness on the maximum displacement

Figures 8 Influence of panel thickness on impact resistance of gradient corrugated sandwich structure

As depicted in Figures 8(a) and 8(b), under identical impact loads, the energy absorption capacity of the corrugated sandwich structure increases with the increase in face sheet thickness. However, an increase in face sheet thickness also significantly increases the total mass of the structure, leading to a decreasing trend in the structure's *SEA*. Concurrently, the increase in face sheet thickness enhances the structural stiffness, resulting in a gradual reduction in the maximum downward displacement of the impactor, thereby improving the structure's resistance to deformation. Thus, while increasing the face sheet thickness can improve the structure's resistance to deformation, it results in a decrease in *SEA*. Consequently, in practical applications, the appropriate face sheet thickness must be selected based on specific requirements.

3.2.4 Effect of Sandwich Wall Thickness on Impact Resistance of Structure

This study aims to investigate the impact of core thickness on the impact resistance performance of corrugated sandwich structures. To this end, impact load simulations were conducted on structures with varying core thicknesses t_c while keeping the thickness of the top, middle, and bottom face sheets constant. The core thicknesses t_c were set to 0.6mm, 0.7mm, 0.8mm, 0.9mm, and 1mm. The simulation results, which detail the specific influence of core thickness on the structural impact resistance performance, are presented in Figure 9.

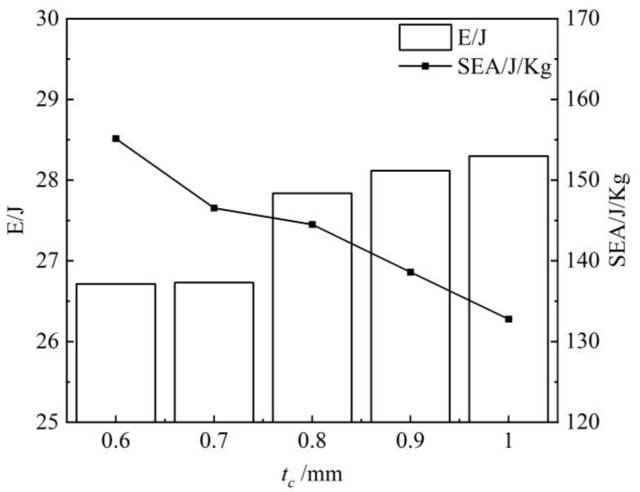

(a) The effect of sandwich wall thickness on energy absorption and specific energy absorption

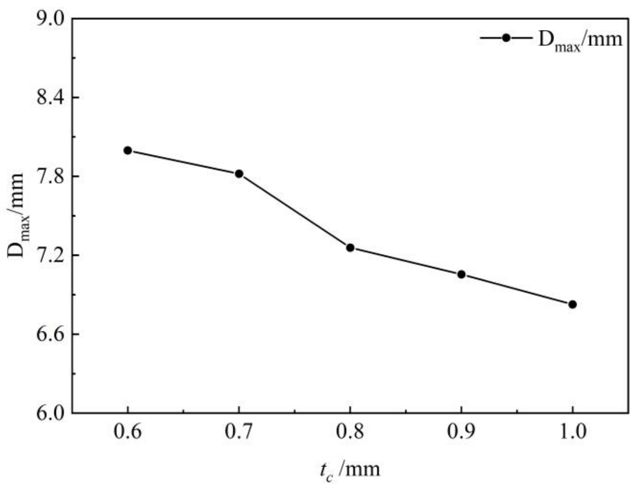

(b) The influence of sandwich wall thickness on the maximum displacement

Figure 9 Effect of sandwich wall thickness on impact resistance of corrugated sandwich structure

Analysis of Figures 9(a) and 9(b) reveals that the impact of core thickness on the structural impact resistance performance is similar to that of face sheet thickness. As the core thickness increases, the overall energy absorption capacity of the structure tends to increase. However, an increase in core thickness also significantly increases the mass of the structure, and despite minimal changes in energy absorption, SEA of the structure decreases. This indicates that simply increasing the core thickness negatively affects the structure's impact resistance performance; while it can enhance the structure's energy absorption, it also increases the structural mass, thereby significantly reducing the structure's SEA. Concurrently, an increase in core thickness leads to greater structural stiffness, and the maximum downward displacement of the impactor decreases with increasing core thickness, enhancing the structure's resistance to deformation. Therefore, increasing the core thickness can improve the structure's resistance to deformation but results in a decrease in SEA. Consequently, in practical applications, the appropriate core thickness must be selected based on specific requirements.

4 Optimization of Variable Gradient Corrugated Sandwich Structure

4.1 Definition of Optimization Problem

To enhance the structural impact resistance during load impact, it is essential to improve the structure's energy absorption capacity and its resistance to deformation. In the context of aerospace structural design, the lightweighting of structures is also a crucial optimization objective. This study selects a 3-6-3 gradient distributed and symmetrically arranged corrugated sandwich structure as the optimized configuration, with face sheet thickness t_f and core thickness t_c as optimization variables. The optimization objectives are to maximize SEA, minimize the maximum downward displacement of the impactor $D_{\max}$, and minimize the total mass of the structure M. A multi-objective optimization of the corrugated sandwich structure is conducted with these defined objectives:

$$\begin{aligned} OPt \quad & Max = SEA(t_f, t_c) \\ & Min = [D_{\max}(t_f, t_c), M(t_f, t_c)] \\ s.t. \quad & 0.8mm \le t_f \le 1.2mm \\ & 0.8mm \le t_c \le 1.2mm \end{aligned} \tag{3}$$

4.2 Optimize the Process

The Polynomial Response Surface Method (RSM) and Kriging method are widely used techniques for constructing surrogate models in engineering. The Polynomial Response Surface Model is favored for its simplicity and effectiveness in addressing highly nonlinear problems [13, 14]. This study utilizes Isight software to employ a multi-objective optimization approach based on the RSM surrogate model to tackle the optimization problem, with the optimization process detailed in Figure 10.

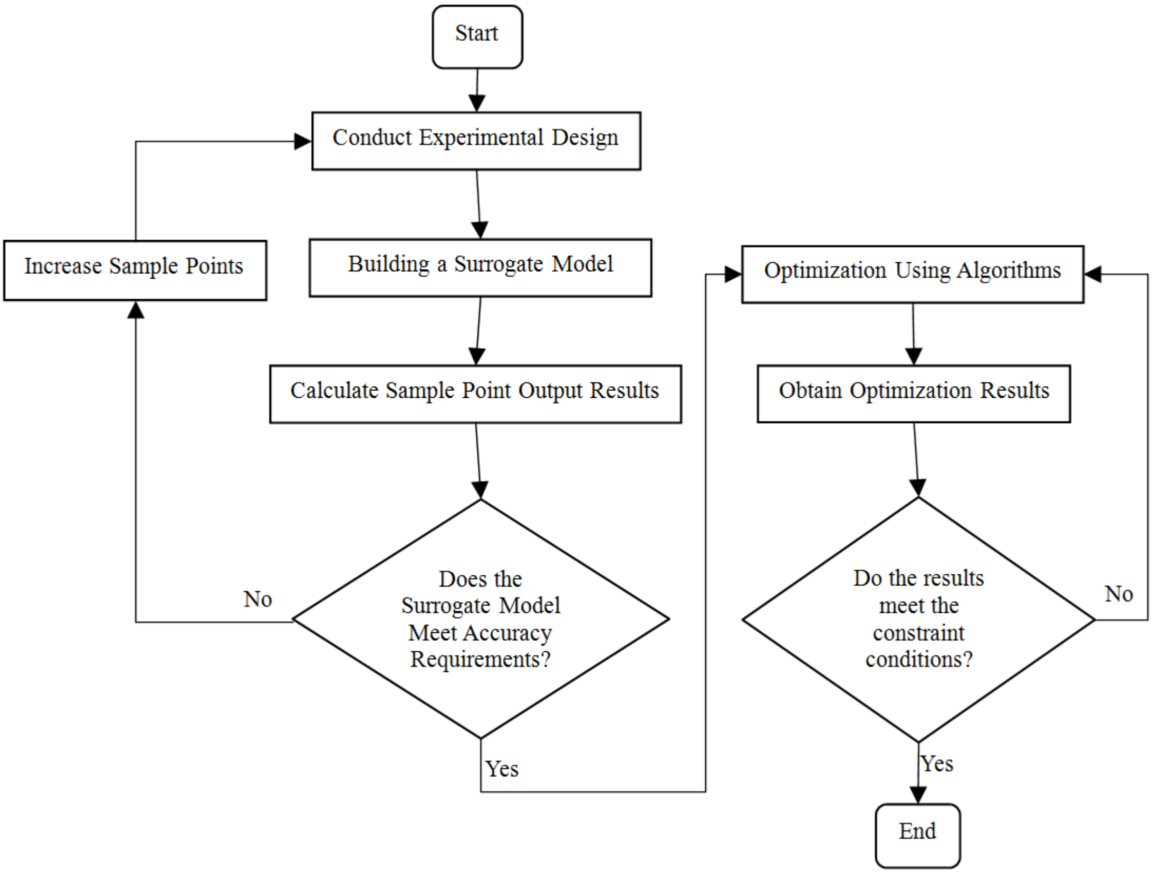

Figure 10 Multi-objective optimization flow chart of variable gradient corrugated sandwich structure

4.3 Proxy Model and Its Accuracy Verification

To determine the coefficients of the RSM and to evaluate the accuracy of the response surface surrogate model, this study employs the Optimal Latin Hypercube Design (OLHD) to generate 15 experimental set sample points for experimental design, and the Latin Hypercube Design (LHD) to generate 10 validation set sample points for accuracy verification. Based on the response results from the OLHD experimental design, a response surface model for the variable gradient symmetrically arranged corrugated sandwich structure was constructed, which includes third-order polynomial response surface equations for SEA, $D_{\max}$, and M, as shown in Equations (4), (5), and (6).

$$SEA = 336.687 - 108.344t_f - 129.805t_c - 43.439t_f^{\ 2} + 6.080t_c^{\ 2} + 47.973t_f t_c + 25.219t_f^{\ 3} + 1.148t_c^{\ 3} \tag{4}$$

$$D_{\max} = 16.049 - 10.616t_f - 7.358t_c + 6.286t_f^{\,2} + 0.0630t_c^{\,2} + 3.094t_f t_c - 1.905t_f^{\,3} + 0.660t_c^{\,3} \quad (5)$$

$$M = 5.473e^{-8} + 0.111t_f + 0.102t_c + 1.156e^{-7}t_f^{\,2} + 7.236e^{-8}t_c^{\,2} + 1.512e^{-10}t_f t_c - 4.075e^{-8}t_f^{\,3} - 2.525e^{-8}t_c^{\,3} \quad (6)$$

In the optimization design process, the accuracy of the surrogate model significantly affects the results of subsequent algorithmic optimization. To ascertain the precision of the surrogate model, this study introduces four evaluation metrics: the coefficient of determination (R-squared, R^2), the Relative Maximum Absolute Error (RMAE), the Relative Average Absolute Error (RAAE), and the Root Mean Square Error (RMSE) [15]. These metrics collectively assess the accuracy of the surrogate model, ensuring the reliability of the optimization process.

$$R^2 = 1 - \frac{\sum_{i=1}^{m}\left(y_i - \hat{y}_i\right)^2}{\sum_{i=1}^{m}\left(y_i - \overline{y}_i\right)^2} \quad (7)$$

$$RAAE = \frac{\sum_{i=1}^{m}\left(y_i - \hat{y}_i\right)^2}{m \times \sqrt{\frac{1}{m-1}\sum_{i=1}^{m}\left(y_i - \overline{y}_i\right)^2}} \quad (8)$$

$$RMAE = \frac{\max\left(\left|y_1 - \hat{y}_1\right|, \left|y_2 - \hat{y}_2\right|, \text{K}, \left|y_m - \hat{y}_m\right|\right)}{\sqrt{\frac{1}{m-1}\sum_{i=1}^{m}\left(y_i - \overline{y}_i\right)^2}} \quad (9)$$

$$RSME = \sqrt{\frac{1}{m}\sum_{i=1}^{m}\left(y_i - \overline{y}_i\right)^2} \quad (10)$$

wherein: y_i - the calculated value of point i of the simulation model;

$\hat{y}_i$ - the function value of point i of the response surface model;

$\overline{y}_i$ - the average value of y_i;

m - the number of sampling points.

When assessing the precision of a surrogate model, it is generally accepted that the closer R^2 value is to 1, and RMAE and RAAE values are, the higher the precision of the model.

The error analysis of the validation set samples within the response surface surrogate model is presented in Table 2. The results indicate that R^2 values are all greater than 0.9, RMAE values are less than 0.3, and RAAE values are less than 0.2, demonstrating that the response surface surrogate model has sufficient accuracy to provide a reliable model for subsequent optimization.

Table 2 Accuracy of response surface surrogate model

Response	R^2	RMSE	RAAE	RMAE
SEA	0.998	0.011	0.007	0.027
$D_{\max}$	0.980	0.044	0.033	0.010
M	1	0	0	0
Evaluation precision	>0.9	<0.2	<0.2	<0.3

4.4 Multi-objective Optimization Results Analysis

The Multi-Island Genetic Algorithm (MIGA) is an optimization algorithm that simulates the natural selection process of survival of the fittest in the natural world, evolving by continuously updating the population to search for the optimal solution and effectively avoiding the trap of local optima. This paper employs a response surface surrogate model, in conjunction with MIGA, to optimize the impact resistance performance of variable gradient corrugated sandwich structures. The Pareto front results for the optimization of the impact resistance of variable gradient corrugated sandwich structures are depicted in Figure 11, with the final optimization results presented in Table 3.

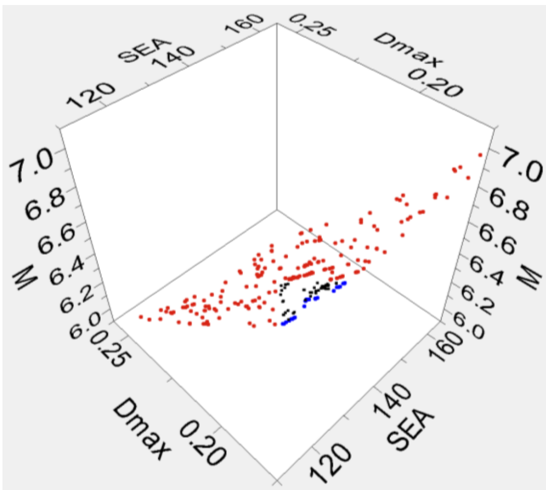

Figure 11 Pareto optimal solution set

Table 3 Optimization results of multi-island genetic algorithm

Optimization parameters	t_f **/mm**	t_c **/mm**	SEA **/J/Kg**	D_{max} **/mm**	M **/Kg**
Optimal results	0.803	1.064	145.85	6.271	0.198

To validate the feasibility of the optimization results, this study conducted a finite element simulation of impact loading on a variable gradient corrugated sandwich structure with specific parameters: t_f of 0.8023mm and t_c of 1.064mm. The optimization results from the response surface surrogate model were compared with the finite element simulation results, as detailed in Table 4. The data in Table 4 indicate that the errors for SEA, D_{max}, and M are all within 1%, thereby confirming the reliability and accuracy of the optimization results.

Table 4 Comparison of optimization results with simulation results

	t_f **/mm**	t_c **/mm**	SEA **/J/Kg**	D_{max} **/mm**	M **/Kg**
Simulation results	0.803	1.064	145.86	6.261	0.198
Predicted results			145.85	6.271	0.198
Error			0.01%	0.01%	0.00%

Table 5 Optimized and comparative model parameter results before and after optimization

Model	**Gradient distribution**	**Arrangement mode**	t_f **/mm**	t_c **/mm**	SEA **/J/Kg**	D_{max} **/mm**	M **/Kg**
Comparison	4-4-4	Regular	1	1	130.57	7.245	0.211
Before optimization	3-6-3	Symmetric	1	1	135.42	6.282	0.213
After optimization	3-6-3	Symmetric	0.803	1.064	145.85	6.271	0.198

Table 5 presents a comparison of the impact resistance performance of the variable gradient corrugated sandwich structure before and after optimization. The optimized variable gradient corrugated sandwich structure showed an increase of 7.71% in SEA, a decrease of 0.33% in D_{max}, and a reduction of 7.16% in M compared to the pre-optimization state. When compared to the 4-4-4 regularly arranged corrugated sandwich structure, the optimized variable gradient symmetrically arranged corrugated sandwich panel structure demonstrated an increase of 11.71% in SEA, a decrease of 13.58% in D_{max}, and a reduction of 6.68% in M. These results indicate that the optimized variable gradient symmetrically arranged corrugated sandwich panel structure can effectively enhance the structural impact resistance performance.

5 Conclusion

To enhance the impact resistance performance of corrugated sandwich structures, this study employed biomimetic variable gradient design methods for optimization. By investigating the influence of structural parameters on the impact resistance performance of corrugated sandwich structures and applying genetic algorithms for multi-objective optimization, the following conclusions were drawn:

(1) Under impact loading, the corrugated sandwich structure designed with a 3-6-3 gradient distribution demonstrates superior energy absorption and deformation resistance compared to the conventional 4-4-4 gradient distribution structure, thus exhibiting enhanced impact resistance performance.

(2) The alteration of the impactor's striking position, the arrangement of the core layers, and the parameters of the sandwich structure, such as face sheet thickness and core thickness, significantly influence the impact resistance performance of the corrugated sandwich structure. By selecting appropriate structural parameters, the impact resistance performance of the structure can be effectively enhanced.

(3) In this study, a response surface approximation model was utilized in conjunction with the MIGA to optimize the design parameters of variable gradient corrugated sandwich structures. The optimization process not only enhanced the efficiency but also significantly improved the structure's impact resistance performance. The results indicated that, compared to the original corrugated sandwich structure, the optimized structure achieved substantial improvements in specific performance metrics.

The findings of this study demonstrate that optimizing the parameters of corrugated sandwich structures can significantly enhance their impact resistance, providing concrete guidance and reference for engineering designs seeking to improve structural resilience against impacts.

References

[1] Sanchez-Saez S, Barbero E, Zaera R, et al. Compression after impact of thin composite laminates [J]. Composites Science & Technology, 2005, 65(13): 1911-1919.

[2] Huang Guibin, Duan Yuechen, Xie Xin. Influence of Impact Angle on Low Speed Flat Head Impact Response of Nomex Honeycomb Sandwich Panels [J]. Composite Materials Science and Engineering, 2022 (10): 25-32.

[3] Qi Jiaqi, Duan Yuechen, Li Cheng, et al. Dynamic response of aluminum honeycomb sandwich panels under low-speed impact [J]. Fiberglass / Composite Materials. 2019 (5): 5-11.

[4] Xin Yajun, Zhang Liwei, Liu Xiaoman, et al. Experimental study on dynamic impact of honeycomb aluminum sandwich panels [J]. Mechanical Strength, 2018, 40 (04): 802-809.

[5] Luo Wei, Xie Wei, Liu Jingxi. Influence of Core Geometric Configuration on Impact Characteristics of Composite Corrugated Sandwich Structures [J]. Journal of Jiangsu University of Science and Technology (Natural Science Edition), 2018, 32 (01): 21-26.

[6] Yin Qun, Wang Hai, Wang Ke, et al. Study on a new type of sandwich double-layer bulkhead structure for ship hulls under penetrating loads [J]. Journal of Jiangsu University of Science and Technology (Natural Science Edition), 2016, 30(02): 103-108.

[7] Fatih U, S H T, Fabrizio S. Low-velocity impact resistance of composite sandwich panels with various types of auxetic and non-auxetic core structures [J]. Thin-Walled Structures, 2021, 163.

[8] Hou S, Shu C, Zhao S, et al. Experimental and numerical studies on multi-layered corrugated sandwich panels under crushing loading [J]. Composite Structures, 2015, 126371-385.

[9] Patek S N, Caldwell R L. Extreme impact and cavitation forces of a biological hammer: strike forces of the peacock mantis shrimp Odontodactylus scyllarus [J]. Journal of Experimental Biology, 2005, 208(19): 3655-3664.

[10] Patek S N, Korff W L, Caldwell R L. Biomechanics: de-adly strike mechanism of a mantis shrimp [J]. Nature, 2004, 428(6985): 819-820.

[11] Weaver J C, Milliron G W, Miserez A, et al. The Stomatopod Dactyl Club: A Formidable Damage-Tolerant Biological Hammer [J]. Science, 2012, 336(6086): 1275-1280.

[12] Chen Yao, Ye Wangjie, Shi Jiayao, et al. Digital design and model verification of Miura origami metamaterial structures [J]. Chinese Journal of Theoretical and Applied Mechanics, 2022, 54(7): 2019-2029.

[13] Huang H, Xu S. Crashworthiness analysis and bionic design of multi-cell tubes under axial and oblique impact loads [J]. Thin-Walled Structures, 2019, 144: 106333.

[14] Fu J, Liu Q, Liufu K, et al. Design of bionic-bamboo thin-walled structures for energy absorption [J]. Thin-Walled Structures, 2019, 135: 400-413.

[15] Chen X, DU w, Liu D. Response surface optimization of biocatalytic biodiesel production with acid oil [J]. Biochemical Engineering Journal, 2008, 40(3): 423-429.